

# Seismic risk assessment of adobe dwellings in Cusco, Peru, based on mechanical procedures

**N. Tarque**

*Istituto Universitario di Studi Superiori - ROSE School, Pavia, Italy  
Civil Engineering Department, Catholic University of Peru, Peru*

**H. Crowley**

*European Centre for Training and Research in Earthquake Engineering, Italy*

**R. Pinho**

*Structural Mechanics Department, University of Pavia, Italy*

**H. Varum**

*Civil Engineering Department, University of Aveiro, Portugal*



## ABSTRACT

A procedure to evaluate the seismic vulnerability of one-storey adobe dwellings located in Cusco (Peru) is presented here. The seismic capacity of these dwellings is based on a mechanical-based approach, where the in-plane and out-of-plane failure mechanisms are taken into account. From a database with the principal geometrical properties of dwellings from Cusco, random populations of buildings were generated through Monte Carlo simulation. The capacity of each random dwelling is expressed as a function of its displacement capacity and period of vibration, and this is evaluated for different damage limit states. The seismic demand has been represented by the displacement spectral shapes computed for different levels of intensity, considering the Peruvian Seismic Code and the Eurocode 8. Finally, from the comparison between capacity and demand, probability of failure have been obtained for different return periods.

*Keywords: seismic risk; adobe dwellings; displacement-based procedures; fragility curves*

## 1. INTRODUCTION

In this work the fragility curves for adobe dwellings placed in Cusco, Peru, have been derived following the Displacement-Based Earthquake Loss Assessment method (*DBELA*, Crowley *et al.* 2006), where the displacement capacity and period of vibration of each random generated building is computed using simple mechanics-based and empirical equations, and compared with the seismic demand to obtain the probability of exceedance. The procedure shown here can be applied to another type of adobe buildings placed in other zones, but taking into account the typical geometrical properties and the seismic hazard of the zone.

## 2. CAPACITY OF ADOBE DWELLINGS

### 2.1. In-plane capacity

From a previous work, the seismic capacity of adobe walls in terms of displacement capacity and period of vibration has been defined (Tarque 2008). The in-plane limit states (*LS*) and period of vibration ( $T_y$ ) were obtained based on a cyclic test carried out at the Catholic University of Peru (Blondet *et al.* 2005) and they were related to the wall height (Table 1). The damping values ( $\zeta$ ) for the limit states were computed based on the hysteretic curves obtained from the test.

The period of vibration for the limit states are computed with Equations 2.1 and 2.2.

$$T_y = C_1 H^{3/4} \quad (2.1)$$

$$T_{LSi} = T_y \sqrt{\mu_{LSi}} \quad (2.2)$$

where  $C_I$  is the period coefficient (close to 0.09, Tarque 2008),  $H$  is the wall height,  $T_y$  is the elastic period of vibration and  $T_{LSi}$  is the period of vibration for LS2, LS3 and LS4.

**Table 1.** In-plane limit states for adobe buildings

Limit state	Description	Drift, $\delta_{LS}$	Damping, $\zeta$ (%)	Ductility, $\mu_{LSi}$
LS1	Operational	0.052%	10	1
LS2	Functional	0.10%	10	2
LS3	Life-safety	0.26%	12	5
LS4	Near or collapsed	0.52%	16	10

## 2.2. Out-of-plane capacity

The out-of-plane capacity has been defined following the work developed by Doherty *et al.* (2002) and Griffith *et al.* (2005), where the ultimate displacement ( $\Delta_u$ ), measured at the top of a cantilever wall, is related to a percentage of the wall thickness ( $t$ ) according to the wall supports and wall axial load, here  $\Delta_u \approx 0.8t$ . The ultimate displacement limit state is affected by a reduction factor  $\phi$  (from 0.8 to 1) to take into account degradation of existing masonry walls (Restrepo-Velez 2004, see Table 2). Besides, two intermediate limit states (LS1 and LS2) were considered according to the author's experience and related to the grade of damage due to vertical cracks at wall corners (Tarque 2008). To compute the displacement capacity for LS1, a 3mm width horizontal crack at the base of one cantilever adobe wall was taken. Assuming that the wall will rotate as a rigid body at the base, a maximum displacement at the top of the wall of about 17mm was computed using 2.45m and 0.44m as the mean values of the wall height and wall thickness from typical houses in Cusco, respectively. The displacement capacity for LS2 was computed directly from the displacement ratio  $\rho_1$  (Table 2, 3) times the mean value of  $\Delta_u$ , resulting in 45mm approximately. The damping value was taken as 5% due to the rocking behaviour.

**Table 2.** Out-of-plane limit states for adobe buildings

Limit state	Displacement capacity for parapets or simply supported walls	$\zeta$ (%)
LS1	$\approx 17\text{mm}$	5
LS2	$\Delta_1 = \rho_1 \cdot \Delta_u$	5
LS3	$\Delta_{LSu} = \phi \cdot \Delta_u$	5

The period of vibration for the limit states are computed with Eq. 2.3 and 2.4.

$$T_{LSi} = 2\pi \sqrt{\frac{\Delta_1}{\lambda g(1 - \rho_2)}} \quad (2.3)$$

$$T_{LSu} = 2\pi \sqrt{\frac{\Delta_{LSu} \cdot \rho_2}{\lambda \phi g(1 - \rho_2)}} \quad (2.4)$$

where  $T_{LSi}$  and  $T_{LSu}$  are the period of vibration for the intermediate and ultimate limit state ( $\Delta_{LSu}$ ), respectively;  $\rho_1$  and  $\rho_2$  are the displacement ratios for the tri-linear model of walls due to out-of-plane forces (Table 3);  $\phi$  is the reduction factor explained before;  $\lambda$  is the collapse multiplier (which depends on the failure mechanism of the wall), and  $g$  is the gravity acceleration.

**Table 3.** Displacement ratios for the tri-linear model (Griffith *et al.* 2003)

State of degradation at cracked joint	$\rho_1 = \Delta_1 / \Delta_u$ (%)	$\rho_2 = \Delta_2 / \Delta_u$ (%)
New	6	28
Moderate	13	40
Severe	20	50

The equations for evaluating the collapse multipliers can be found in Restrepo-Velez (2004). For example, for overturning of walls (Figure 1) the Eq. 2.5 is used to compute the collapse multiplier.

$$\lambda = \frac{\frac{t^2 L}{2} + \beta \cdot \Omega_{pef} \frac{h_s}{3} \mu_s \cdot s \cdot b \frac{(r+1)}{2} + \frac{K_r L t}{2}}{h_s \left( \frac{tL}{2} + K_r L \right)} \quad (2.5)$$

where  $t$  and  $L$  are the thickness and length of the front walls,  $\beta$  is the number of edge and internal perpendicular walls,  $\Omega_{pef}$  is a partial efficiency factor to account for the limited effect of the friction,  $h_s$  is the height of the failing portion of the wall,  $\mu_s$  is the friction coefficient,  $s$  is the staggering length (normally it is the brick half length),  $b$  is the thickness of the brick units,  $r$  is the number of courses within the failing portion (assuming courses in the rocking portion);  $K_r$  is the overburden load, in which  $Q_r$  is the load per unit length on the top of the front wall, and  $\gamma_m$  is the volumetric weight of masonry.

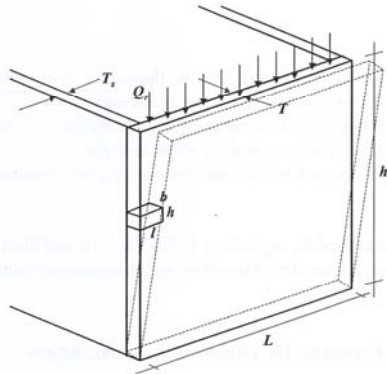


**Figure 1.** Failure mechanism for out-of-plane (Restrepo-Velez 2004).

### 3. GEOMETRICAL DATABASE

In 2004, Blondet *et al.* (2004) carried out a building-to-building survey in Cusco, a city located at the Peruvian highland. According to the last census (INEI 2007), Cusco has around 76% of houses built in adobe (Figure 2) or tapial (rammed earth) and at least 54% of them are of 1-storey. The data which was collected included the dimensions of walls and bricks, the height of gable, number of rooms, number of openings, etc. With that data it was possible to define the mean values and standard deviations of these geometrical properties. For example, it was found that the mean wall thickness of adobe buildings in Cusco is 0.44m, and the mean wall height is 2.45m for 1-storey buildings. The thickness of the wall is fairly uniform amongst the buildings analysed, confirmed by the low standard deviation.



**Figure 2.** Adobe buildings in Cusco, Blondet *et al.* (2004).

The variability of each of the parameters in this study (*i.e.* wall lengths, wall heights, adobe brick dimensions, etc.) were represented by histogram plots which were then fit to a probability density function (PDF). Figure 3 shows the histograms and the best-fit PDF for some of the geometrical parameters.

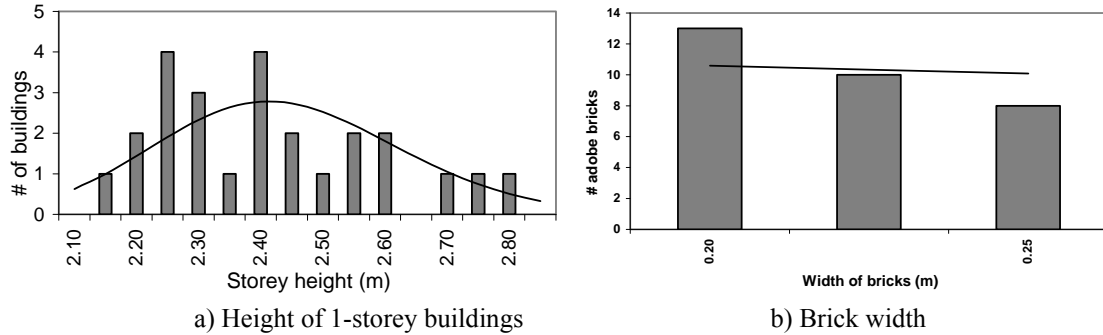


**Figure 3.** Histograms and PDFs for the mean geometrical properties.

### 3.1. Generation of random data

With Monte Carlo simulation it was possible to generate an artificial stock of 1000 buildings (Crowley *et al.* 2006). The input data (based on the statistics of the 30 adobe dwellings; Blondet *et al.* 2004) was represented by the mean and standard deviation values of the principal geometrical properties (Table 4) and by the best fit for the probability density functions (*e.g.* lognormal, normal, uniform and discrete distributions). Some values as the overburden load for typical adobe dwellings were taken from Tejada (2001). The standard deviation values for the limit states have been established up to 20% of the mean value to take into account the variability of parameters. Some parameters can be given just as integer (Table 5). Then, the displacement capacity and the respective period of vibration for different limit states for each of the 1000 randomly generated buildings was generated (Figure 4).

**Table 4.** Random variables used in DBELA for the definition of structural capacity of adobe dwellings

Description	Variable	Mean ( $\mu$ )	Standard deviation ( $\sigma$ )	Distribution
<i>In-plane failure mechanism</i>				
Inter-storey height (m)	$h_p$	2.45	0.21	Lognormal
Pier height (m)	$h_{sp}$	2.45	0.21	Lognormal
Period coefficient	$C_1$	0.088	0.004	Normal
Drift limit state 1	LS1	0.00052	0.0001	Lognormal
Drift limit state 2	LS2	0.001	0.0002	Lognormal
Drift limit state 3	LS3	0.0026	0.00052	Lognormal
Drift limit state 4	LS4	0.0052	0.001	Lognormal
<i>Out-of-plane failure mechanism</i>				
Wall width (m)	$t$	0.44	0.04	Lognormal
Wall length (m)	$L$	4.53	0.59	Lognormal
Staggering length (m)	$s$	0.103	0.008	Lognormal
Thickness of brick units (m)	$b$	0.44	0.004	Lognormal
Height of brick units (m)	$h$	0.152	0.01	Lognormal
Overburden load (kN/m)	$Q_r$	6.7	---	---
Specific weight (kN/m <sup>3</sup> )	$\gamma_m$	18	---	---
Reduction factor for $\Delta_u$	$\phi$	0.85	0.05	Normal
Friction coefficient	$\mu_s$	0.80	---	---
$\Delta_1/\Delta_u$	$\rho_1$	0.12	0.01	Normal
$\Delta_2/\Delta_u$	$\rho_2$	0.4	---	---
Limit state 1 (m)	LS1	0.017	0.001	Normal
# of edge and internal orthogonal walls	$\beta$	See Table 5a		Discrete
# of courses within the storey height	$r$	See Table 5b		Discrete

**Table 5.** (a) # of edge and internal orthogonal walls; (b) # of courses within the storey height

a)	Number	Total	Cumulative	b)	Number	Total	Cumulative
	2	24	0.40		12	1	0.04
	3	22	0.77		13	1	0.08
	4	2	0.97		14	7	0.35
	5	2	1.00		15	22	0.77
					16	2	0.85
					17	4	1.00

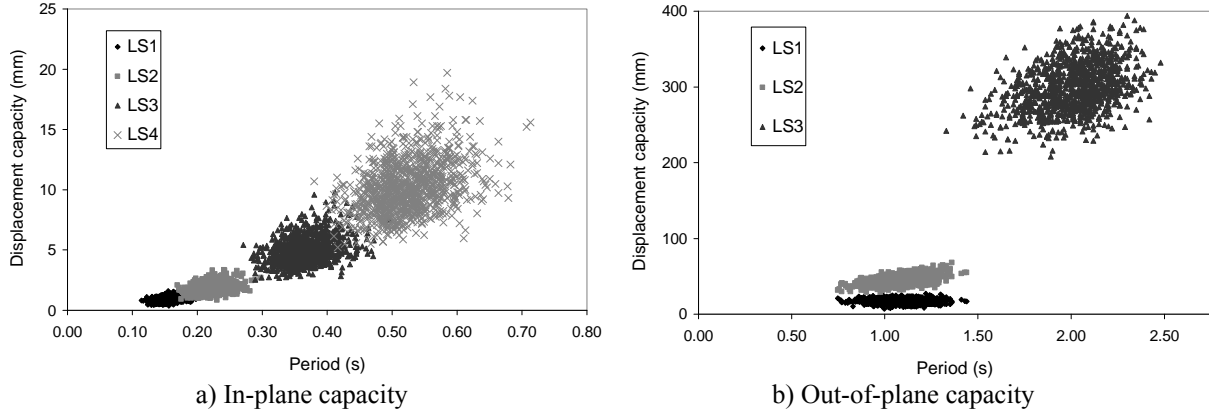


**Figure 4.** Seismic capacity of adobe walls for different limit states.

#### 4. SEISMIC DEMAND

The seismic demand has been represented by many Displacement Response Spectra (DRS) computed from two code spectrum: the Peruvian Seismic Code and the Eurocode 8. A soil type with  $180 < V_{s30} < 360 \text{ m/s}^2$  was used for Cusco.

##### 4.1. Peruvian Seismic Code

The Equations 4.1 and 4.2 are used to evaluate the acceleration response spectrum (ARS) with the Peruvian seismic code (VIVIENDA/SENCICO 2003):

$$S_a = \frac{Z \cdot U \cdot S \cdot C}{R} g \quad (4.1)$$

$$C = 2.5 \cdot \frac{T_p}{T} \leq 2.5 \quad (4.2)$$

where  $S_a$  are the values of the spectral ordinates;  $Z$  is the expected PGA;  $U$  is a factor that depends on the importance of the building;  $S$  is the soil factor;  $C$  is the seismic amplification factor and should be less than 2.5;  $R$  is a reduction factor; and  $T_p$  is the period corresponding to the end of the plateau zone. For houses,  $U$  is equal to 1 and the soil type in Cusco has been classified as intermediate soil regarding the Peruvian Seismic Code, which is close to the soil type  $C$  given by EC8, and thus the soil factor is equal to 1.2 and  $T_p$  is 0.6s for intermediate soils. The acceleration spectral ordinate for  $T = 0\text{s}$  does not give the PGA value (as is the case in the EC8 spectrum, CEN 2005). For this reason the Acceleration Response Spectra (ARS) shape starts directly from a plateau zone up to  $T_p$ .

Since the Peruvian code does not specify the corner period for displacement response spectra, from where the displacement is constant, the acceleration spectra have been directly transformed to displacement spectra even after to 2s. Since adobe walls have damping values different than 5%, the acceleration response spectra are affected by the damping correction factor  $\eta$  (Equation 4.3, Priestley

et al. 2007).

$$\eta = \sqrt{\frac{7}{2 + \xi}} \quad (4.3)$$

where the equivalent viscous damping  $\xi$  is given in %.

#### 4.2. Eurocode 8

The acceleration spectral shape specified by EC8 (CEN 2005) has been anchored to increasing levels of PGA to generate a set of acceleration response spectra which have then been multiplied by  $(T/2\pi)^2$  to obtain the displacement response spectra. Following the recommendations of EC8, the displacement spectra have been taken as constant after 2s. The following equations allow to compute the ARS.

$$0 \leq T < T_B : S_e(T) = a_g \cdot S \left( 1 + \frac{T}{T_B} \cdot (\eta \cdot 2.5 - 1) \right) \quad (4.4)$$

$$T_B \leq T < T_C : S_e(T) = a_g \cdot S \cdot \eta \cdot 2.5 \quad (4.5)$$

$$T_C \leq T < T_D : S_e(T) = a_g \cdot S \cdot \eta \cdot 2.5 \cdot \frac{T_C}{T} \quad (4.6)$$

$$T_D \leq T \leq 4s : S_e(T) = a_g \cdot S \cdot \eta \cdot 2.5 \cdot \frac{T_C \cdot T_D}{T^2} \quad (4.7)$$

where  $S_e$  are the values of the spectral ordinates;  $a_g$  is the PGA value;  $S$  is the soil factor;  $T_B$ ,  $T_C$  and  $T_D$  are the characteristic periods of the spectral shape and depends on the ground type and  $\eta$  is the damping correction factor (Eq. 4.3) that should be 1 for the elastic response spectra.

The parameters given by Eurocode 8 were taken assuming that earthquakes in Cusco have magnitudes higher than  $M_w$  5.5 (Erickson *et al.* 1954). The soil type selected was *C* ( $180 < V_{s30} < 360 \text{m/s}^2$ ), which means soil factor  $S = 1.15$ . The resulting values for  $T_B$ ,  $T_C$ ,  $T_D$  were 0.2, 0.6 and 2s, respectively.

Figure 5 shows two acceleration and related displacement spectral shapes computed from the two seismic design codes considering  $a_g \cdot S = 0.17g$ . It seems that the spectral shapes from both codes are similar, so the computed fragility curves will give similar results from both seismic codes. However, it should be important to analyze other spectral shapes from Ground Motion Prediction Equations (GMPE) in order to see the influence of different spectral shapes on the fragility curves.

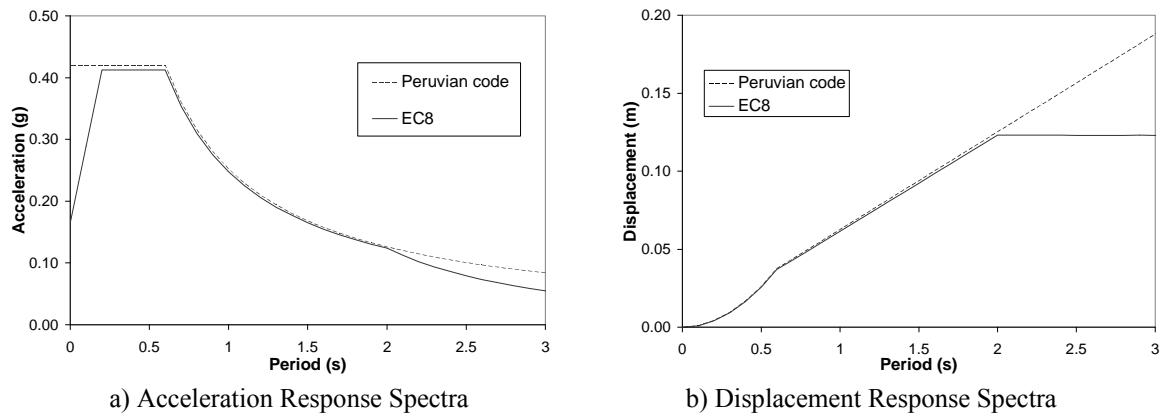
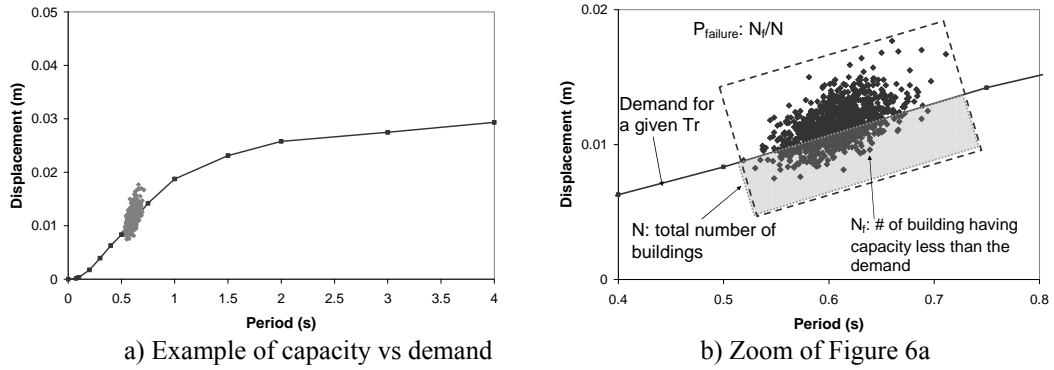


Figure 5. Seismic demand.

## 5. FRAGILITY CURVES FOR ADOBE DWELLINGS IN CUSCO

The construction of the fragility curves starts with the computation of the probability of exceedance, which is obtained for the first limit state by calculating the ratio between the number of dwellings with a displacement capacity lower than the displacement demand and the total number of dwellings (Figure 6). The probability of exceeding for subsequent limit states is obtained from the ratio between the number of dwellings that exceeded the previous limit state and that still have a displacement capacity lower than the displacement demand at this next limit state, and the total number of dwellings. This evaluation can be repeated for a number of displacement response spectra with increasing levels of peak ground acceleration (PGA) and plotted to produce fragility curves.



**Figure 6.** Evaluation of the probability of exceedance for fragility curves (Tarque 2008).

The elastic DRS should be multiplied by the modification factor  $\eta$  in order to take into account the higher levels of damping for the in-plane analysis. For the out-of-plane, the elastic DRS should be scaled by 1.5 for comparison with the displacement capacity (Griffith *et al.* 2005). The adobe buildings generated herein have in-plane limit state periods of vibration between 0.12 and 0.7s and out-of-plane limit state periods of vibration between 0.75 and 2.5s. Fragility curves for adobe dwellings in Cusco are showed in Figure 7.

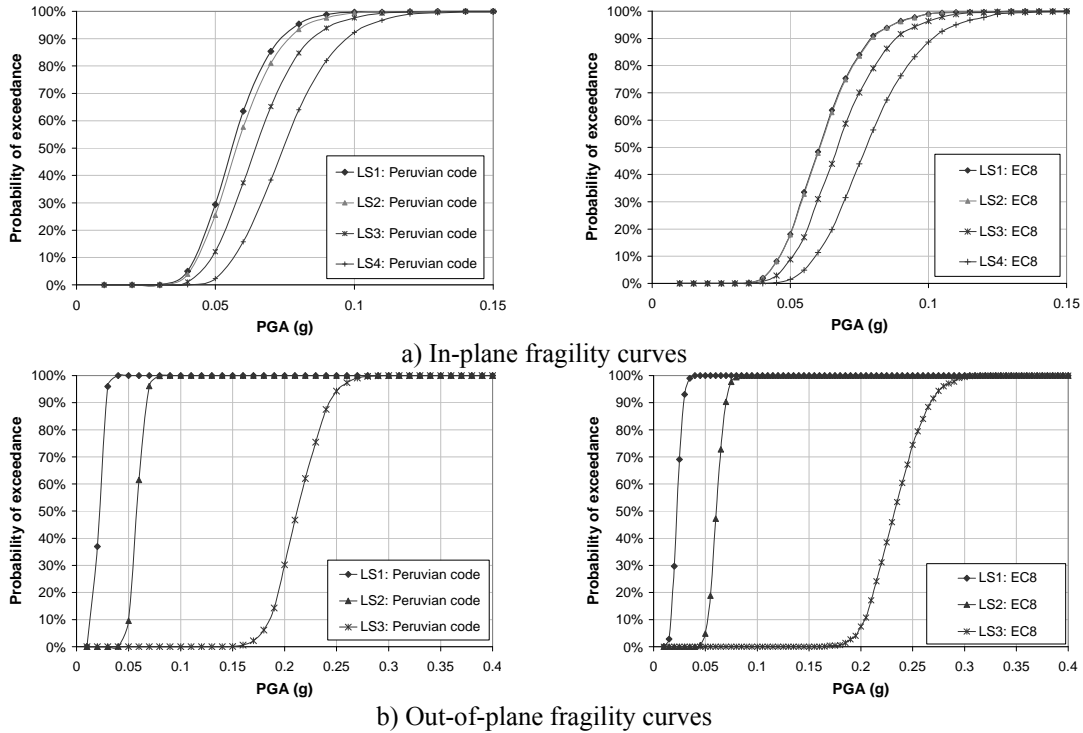


**Figure 7.** Fragility curves considering the Peruvian code and the Eurocode 8.

## 6. CONCLUSIONS

Fragility curves for typical adobe dwellings in Cusco have been derived here following the *DBELA* procedure. Data from 30 surveyed dwellings were used to compute the mean, standard deviation and probability density functions of relevant geometrical properties. Using Monte Carlo simulation it was possible to generate 1000 buildings stock and to evaluate the seismic capacity, in-plane and out-of-plane, of the adobe dwellings. The seismic hazard was represented by a number of displacement response spectra. The probability of exceedance, considering each limit state, was computed by comparing the capacity with the demand.

The spectral shapes from both seismic codes adopted give close spectral ordinates until the corner period specified by the EC8. The Peruvian seismic code does not specify any corner period; therefore, the ordinates from the DRS increases in value either after the corner period. This aspect influences the fragility curves for LS3 of the out-of-plane behaviour due to the high period values for LS3. For the in-plane, both seismic codes give close fragility curves.

The computed fragility curves show the high seismic vulnerability of adobe dwellings. It seems that for events with PGA higher than 0.1g, some in-plane cracking is expected to see with vertical damage at corners of walls. For events with PGA higher than 0.25g, a complete overturning of walls due to out-of-plane failure may occur, and the small blocks formed by diagonal cracking could even overturn. The shape of the DRS influences on the fragility curves, so other spectral shapes should be taken into account in the analysis.

## REFERENCES

- Blondet, M., Tarque, N., Acero, J. (2004). Study of the seismic vulnerability of non-engineering buildings located at the Peruvian Highlands, in Spanish, Joint Project SENCICO-PUCP, Catholic University of Peru, Lima, Peru.
- Blondet, M., Madueño, I., Torrealva, D., Villa-García, G., Ginocchio, F. (2005). Using industrial materials for the construction of safe adobe houses in seismic areas. *Earth Build 2005Conference*, Sydney, Australia.
- CEN, (2005). Design of Structures for Earthquake Resistance, Part 1: General rules, seismic action and rules for buildings, Eurocode 8. ENV-1998-1-1, Comité Européen de Normalisation, Brussels, Belgium.
- Crowley, H., Pinho, R., Bommer, J.J., and Bird, J. (2006). Development of a Displacement Based Method for Earthquake Loss Assessment. European School for Advanced Studies in Reduction of Seismic Risk (ROSE School), IUSS Press, Pavia, Italy.
- Doherty, K., Griffith, M.C., Lam, N., and Wilson, J. (2002). Displacement-based seismic analysis for out-of-plane bending of unreinforced masonry wall, *Journal of Earthquake Engineering and Structural Dynamic* **31**, 833-850.
- Eriksen, G., Fernandez, J., and Silgado, E. (1954). The Cusco, Peru, Earthquake of May 21, 1950. *Bulletin of the Seismological Society of America*, No. **2**, vol. **44**, 97-112.
- Griffith, M.C., Magenes, G.M., Melis, G., and Picchi, L., (2003). Evaluation of Out-of-Plane Stability of Unreinforced Masonry Walls Subjected to Seismic Excitation, *Journal of Earthquake Engineering* **7**, special Issue No. **1**, 141-169.
- Griffith, M.C., Lam, M., and Wilson, J. (2005). Displacement-based assessment of the seismic capacity of Unreinforced Masonry walls in bending, *Australian Journal of Earthquake Engineering*, Vol. **6**, No. **2**.
- INEI. Census 2007, (2007). National Institute of Statistic and Informatics, Lima, Peru. Available at October 2009 from [www.inei.gob.pe](http://www.inei.gob.pe).
- Priestley, M.J.N., Calvi, G.M., and Kowalsky, M.J. (2007). Displacement-Based Seismic Design of Structures, IUSS Press. Pavia, Italy.
- Restrepo-Velez, L. (2004). Seismic Risk of Unreinforced Masonry Buildings, Doctoral Thesis, European School for Advanced Studies in Reduction of Seismic Risk (ROSE School). University of Pavia, Pavia, Italy.
- Tarque, N. (2008). Seismic Risk Assessment of Adobe Dwellings. European School for Advanced Studies in Reduction of Seismic Risk (ROSE School), University of Pavia, Pavia, Italy. Available at October 2009 from: [http://www.roseschool.it/index.php?option=com\\_docman&task=doc\\_download&gid=183&mode=view](http://www.roseschool.it/index.php?option=com_docman&task=doc_download&gid=183&mode=view)
- Tejada, U. (2001). Buena Tierra, apuntes para el diseño y construcción con adobe (in Spanish), CIDAP: Centre of Researching, Documentation and Consultant Assistance, Lima, Peru.
- VIVIENDA/SENCICO, NTE E.030 – Technical Code for Buildings, (2003). Earthquake Resistant Design (in Spanish), Ministry of Housing, Construction and Sanitation, SENCICO. Peru.